Clinical Pharmacology & Biopharmaceutics

Trivedi et al., Clin Pharmacol Biopharm 2015, 4:2
DOI: 10.4172/2167-065X.1000138

Research Article Open Access

Evaluation of the Impact of Biofield Treatment on Physical and Thermal Properties of Casein Enzyme Hydrolysate and Casein Yeast Peptone

Trivedi MK, Nayak G, Patil S*, Tallapragada RM, Jana S and Mishra R

Trivedi Global Inc., 10624 S Eastern Avenue Suite A-969, Henderson, NV 89052, USA

Abstract

In the present study, the influence of biofield treatment on physical and thermal properties of Casein Enzyme Hydrolysate (CEH) and Casein Yeast Peptone (CYP) were investigated. The control and treated samples were characterized by Fourier transform infrared (FT-IR) spectroscopy, differential scanning calorimetry (DSC), Thermo Gravimetric Analysis (TGA), particle size and surface area analysis. The FTIR results revealed that biofield treatment has caused reduction of amide group (amide-I and amide-II) stretching vibration peak that is associated with strong intermolecular hydrogen bonding in treated CEH as compared to control. However, no significant changes were observed in FTIR spectrum of treated CYP. The TGA analysis of treated CEH showed a substantial improvement in thermal stability which was confirmed by increase in maximum thermal decomposition temperature (217˚C) as compared to control (209˚C). Similarly, the treated CYP also showed enhanced thermal stability as compared to control. DSC showed increase in melting temperature of treated CYP as compared to control. However the melting peak was absent in DSC of treated CEH which was probably due to rigid chain of the protein. The surface area of treated CEH was increased by 83% as compared to control. However, a decrease (7.3%) in surface area was observed in treated CYP. The particle size analysis of treated CEH showed a significant increase in average particle size (d_{50}) and d_{99} value (maximum particle size below which 99% of particles are present) as compared to control sample. Similarly, the treated CYP also showed a substantial increase in d_{50} and d_{99} values which was probably due to the agglomeration of the particles which led to formation of bigger microparticles. The result showed that the biofield treated CEH and CYP could be used as a matrix for pharmaceutical applications.

Keywords: Casein enzyme hydrolysate; Casein yeast peptone; Biofield treatment; FT-IR; TGA; DSC; Particle size and Surface area

Abbreviations: CEH: Casein Enzyme Hydrolysate; CYP: Casein Yeast Peptone; FT-IR: Fourier Transform Infrared Spectroscopy; TGA: Thermogravimetric Analysis; DSC: Differential Scanning Calorimetry; DTG: Derivative Thermogravimetry BET: Brunauer-Emmett-Teller; DDS: Drug Delivery Systems.

Introduction

Over the last few decades, there has been continuous interest in biodegradable polymers for pharmaceutical and biomaterial applications [1]. Biodegradable polymers can be either synthetic or natural polymers. The synthetic polymers are more popular than their natural counterparts due to their excellent mechanical properties which can be used for biomedical applications. However the synthetic polymers are associated with toxicity problems which may cause problems during their intended medical use. Natural polymers are generally regarded as safe compared to synthetic polymers. Hence the natural polymers have clear advantages as drug delivery systems (DDS) [2]. Recently, protein based therapeutics, due to their excellent properties such as emulsification, foaming, gelling, and water holding ability have gained significant attention as DDS [3-6]. Moreover, the food proteins have their inherent ability to interact with wide range of bioactive compounds via functional groups present on their polypeptide structure. Hence, this offers the reversible binding of active molecules and protects them until their safe release in the human body [7,8]. Additionally, proteins are metabolizable; hydrolysis of the proteins by digestive enzymes releases the bioactive peptides that may cause a number of beneficial effects such as cardiovascular, endocrine, immune and nervous system [9,10].

Milk proteins are natural vehicles and widely explored in food industries due to their inherent nutritional and functional properties. Casein is a main structural component of milk, where it accounts for 80% of total proteins content. Casein has been utilized in the production of food, pharmaceutical formulations and cosmetics. The interesting structure and physicochemical properties allows it to be used in DDS [11]. The casein has fascinating properties such as binding of ions and small molecules, excellent emulsification, surface active, gelation and water binding capacities.

Hydrolysation of protein makes changes in the composition of potential groups; hydrophobic properties and functional characteristics [12]. For example CEH is a protein that is rapidly absorbed and digested similar to whey protein. Enzyme hydrolysis was recently used to modify the protein structure in order to enhance the functional properties of proteins. However, these chemical and enzymatic treatments might induce denaturation of protein which directly affects its functional properties.

Bioelectromagnetism is an area which studies the interaction of living biological cells and electromagnetic fields. Researchers have demonstrated that short lived electrical current or action potential exists in several mammalian cells such as neurons, endocrine cells and muscle cells as well as some plant cells. An Italian physicist Luigi

***Corresponding author:** Shrikant Patil, Trivedi Global Inc., 10624 S Eastern Avenue Suite A-969, Henderson, NV 89052, USA, Tel: +1 602-531-5400; E-mail: publication@trivedieffect.com

Received June 10, 2015; **Accepted** June 29, 2015; **Published** July 06, 2015

Citation: Trivedi MK, Nayak G, Patil S, Tallapragada RM, Jana S, et al (2015) Evaluation of the Impact of Biofield Treatment on Physical and Thermal Properties of Casein Enzyme Hydrolysate and Casein Yeast Peptone. Clin Pharmacol Biopharm 4: 138. doi:10.4172/2167-065X.1000138

Copyright: © 2015 Trivedi MK, et al. This is an open-access article distributed under the terms of the Creative Commons Attribution License, which permits unrestricted use, distribution, and reproduction in any medium, provided the original author and source are credited.

Galvani first time observed this phenomenon in a frog where he had been working on static electricity [13]. Similarly it was believed that electromagnetic field exists around the human body and the evidence was found using some medical technologies such as electromyography, electrocardiography, and electroencephalogram. This field is known as biofield and the exposure of the said biofield has been referred hereinafter as Biofield treatment.

Recently, biofield treatment was used to modify the physical, atomic and thermal properties of various ceramic, metals and carbon allotropes [14-21]. Mr. Trivedi is known to transform these materials using his biofield. The biofield treatment has also improved the production and quality of various agricultural products [22-25]. Moreover, the biofield has resulted into altered antibiotic susceptibility patterns and the biochemical characteristics of various bacteria [26-28]. Exposure to the said biofield has caused an enhancement in growth and anatomical characteristics of herbs like *Pogostemon cablin* that is commonly used in perfumes, in incense/insect repellents, and alternative medicine [29]. In this study, the effects of biofield treatment on two protein based organic compounds (CEH and CYP) are studied and their physicochemical properties are evaluated.

Materials and Methods

The casein enzyme hydrolysate and casein yeast peptone were procured from HiMedia Laboratories Pvt. Ltd. India. The samples were grouped into two parts; one was kept as a control sample, while the remaining sample was subjected to Mr. Trivedi's biofield treatment and coded as treated sample. After that, all the samples (control and treated) were characterized with respect to FTIR, DSC, TGA, particle size and surface area analysis.

Characterization

Fourier Transform Infrared (FTIR) spectroscopy: The infrared spectra of CEH and CYP (control and treated) were recorded on FT-IR spectrometer, (Perkin Elmer, USA).

The IR spectrum was recorded in the range of 4000-500 cm^{-1}.

Particle size analysis: The average particle size and particle size distribution were analyzed by using Sympetac Helos-BF Laser Particle Size Analyzer with a detection range of 0.1 micrometer to 875 micrometer. Average particle size (d_{50}) and d_{99} (maximum particle size below which 99% of particles) were computed from laser diffraction data table. The d_{50} and d_{99} value were calculated using the following formula.

Percentage change in d_{50} size = 100 × (d_{50} treated- d_{50} control)/ d_{50} control

Percentage change in d_{99} size = 100 × (d_{99} treated- d_{99} control)/ d_{99} control

Surface area analysis: The surface area of CEH and CYP were characterized by using surface area analyzer, SMART SORB 90 BET (Brunauer-Emmett-Teller), which had a detection range of 0.1-100 m^2/g.

Differential scanning calorimetry (DSC) study: The CEH and CYP (control and treated) were used for DSC study. The samples were analyzed by using a Pyris-6 Perkin Elmer DSC on a heating rate of 10°C/min under oxygen atmosphere.

Thermogravimetric analysis (TGA): Thermal stability of CEH and CYP (control and treated) were analyzed by using Metller Toledo simultaneous TGA. The samples were heated from room temperature to 400°C with a heating rate of 5°C/min under oxygen atmosphere.

Results and Discussion

FTIR spectroscopy:

Figure 1a and 1b showed the FTIR spectrum of control and treated CEH, respectively. The FTIR spectrum of control CEH showed (Figure 1a) an important absorption peaks at 3215 cm^{-1}, 2974 cm^{-1} which were attributed to -OH and -CH stretching vibration peaks respectively. Other absorption peaks were observed at 1654 cm^{-1} and 1596 cm^{-1} due to amide-I and amide-II stretching vibration peaks. The spectrum showed peaks at 1078 cm^{-1} which was responsible to -OH bending vibration peaks. The treated CEH showed (Figure 1b) shifting of the -OH/-NH stretching and amide (amide-I and amide-II) peaks toward lower wavenumbers. The -OH stretching vibration peak was shifted to 3199 cm^{-1} and amide group peaks were shifted to lower wavenumber 1633 cm^{-1} and 1587 cm^{-1} respectively. This showed that biofield treatment has induced strong intermolecular hydrogen bonding in treated CEH structure. It was previously shown that hydrogen bonding lowered the frequency of stretching vibrations in proteins, since it lowers the restoring force, however increases the frequency of bending vibrations since it produces an additional restoring force [30,31]. Additionally it was shown that hydrogen bonding in -NH group lowers the stretching vibration by 10 to 20 cm^{-1} [32]. Hence in treated CEH, the amide-I band lowered by 21 cm^{-1} and amide-II lowered by 13 cm^{-1} provided a strong proof of hydrogen bonding in the treated sample.

The Figure 2a and 2b shows the FTIR spectrum of control and treated CYP powder. FTIR spectrum of treated and control powder shows (Figure 2a) slight reduction in the hydrogen bonded -OH stretching of treated sample as compared to control. The control CYP sample showed 1635 and 1589 cm^{-1} which were due to amide-I and amide-II stretching vibration peaks. The treated sample showed (Figure 2b) minimal changes in wavenumber of -OH (3060 cm^{-1}) , amide-I (1687 cm^{-1}) and amide-II (1585 cm^{-1}). The results confirmed that biofield treatment has induced the structural changes in the treated samples.

Particle size and surface area analysis

The particle size analysis results of CEH and CEP (control and treated) are depicted in Figures 3 and 4. The average particle size

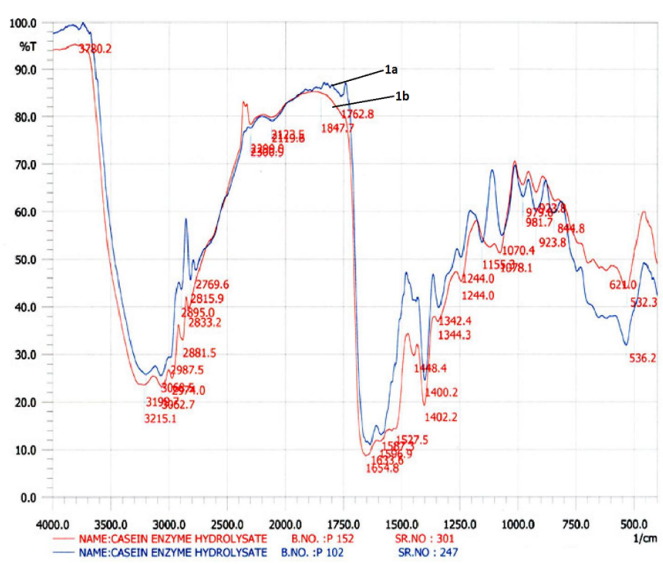

Figure 1: FTIR spectrum of (a) Control casein enzyme hydrolysate (b) Treated casein enzyme hydrolysate.

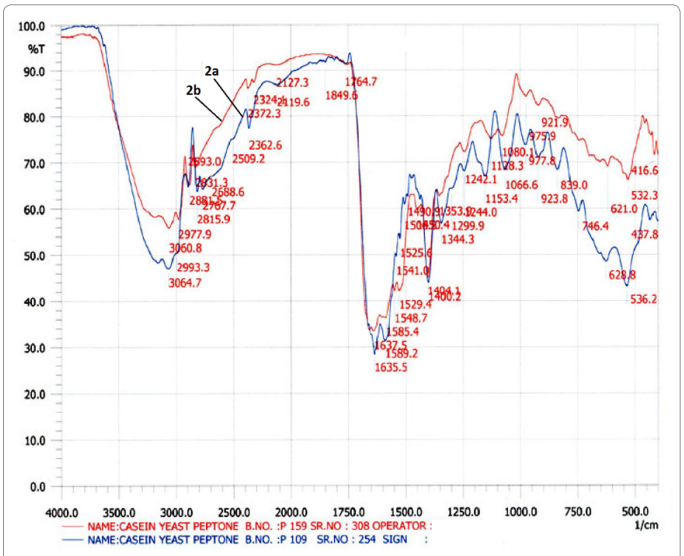

Figure 2: FTIR spectrum of (a) Control casein yeast peptone (b) Treated casein yeast peptone.

(d_{50}) and d_{99} values were calculated from the particle size distribution results (Figure 3). The control CEH showed d_{50} value of 11.88 µm and it has found increased to 12.6 µm in treated sample. The d_{99} value was also increased in treated sample (136.74 µm) as compared to control (115.16 µm). The percentage average particle size, d_{50} and d_{99} of the treated CEH were increased (6.1 and 18.7%) substantially as compared to control (Figure 4).

Whereas, in treated sample of casein yeast peptone (12.61 µm), the d_{50} value has been found increased in comparison with control (10.86 µm). Nonetheless, most significant result was observed in d_{99} value of treated sample of CYP which was found to be 317.52 µm as compared to 143.4 µm in control sample. In treated, the average particle sizes, d_{50} and d_{99} of CYP were found increased by 16.1% and 121.4% respectively (Figure 4).

The surface area was analyzed by BET analysis and the results are presented in Table 1. The surface area of treated CEH (1.004 m^2/g) showed significant improvement as compared to control sample (0.5459 m^2/g). After calculation, the percentage change in surface area was found to be increased by 83.9% in the treated sample of CEH. Contrarily the treated CYP (1.12 m^2/g) showed a decrease in surface area by 7.3% as compared to control sample (1.21 m^2/g). This result can be correlated with increased particle size results of CYP. The surface area and particle size changes are usually opposite to each other, i.e. smaller the particles size, larger the surface area and vice versa [33-35]. Hence, we conclude that increase in particle size substantially reduced the surface area of treated CYP as compared to control sample.

Differential Scanning Calorimetry (DSC)

DSC is a popular technique for investigating the glass transition, melting nature and change in specific heat capacity of materials. The DSC thermogram of control and treated CEH is presented in Figure 5a and 5b. The control CEH sample showed (Figure 5a) an endothermic peak at 140°C which was probably due to bound water with the protein sample. The thermogram also showed a very broad endothermic inflexion at 198°C which was responsible for its melting temperature. The broad peak was probably due to associated water with the sample. DSC of treated CEH showed (Figure 5b) no thermal transition in its thermogram. This was probably due to the highly rigid nature of the treated protein network which was not melted even on the higher temperature. It may be correlated with good thermal stability of the treated sample. Based on the results, we postulate that biofield may have acted directly upon amorphous regions of protein hydrolysate and induced the atoms to come together that led to the formation of a long range order. This may have caused higher crystallinity and ordered regions which probably required more energy in order to break the chains.

The DSC thermogram of CYP (control and treated) powders are presented in Figure 6a and 6b. The control sample showed (Figure 6a) an endothermic peak at 144°C. However the DSC thermogram of treated CYP showed (Figure 6b) a broad endothermic peak at 191°C which was associated with its melting temperature. This showed the increased thermal stability of the CYP after biofield treatment.

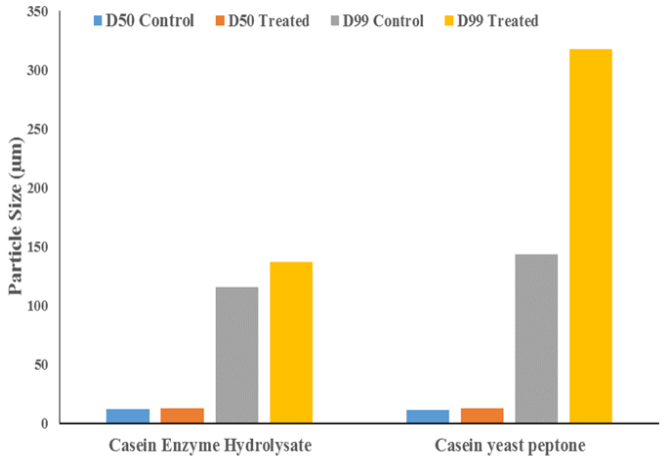

Figure 3: Particle sizes of Control and Treated samples.

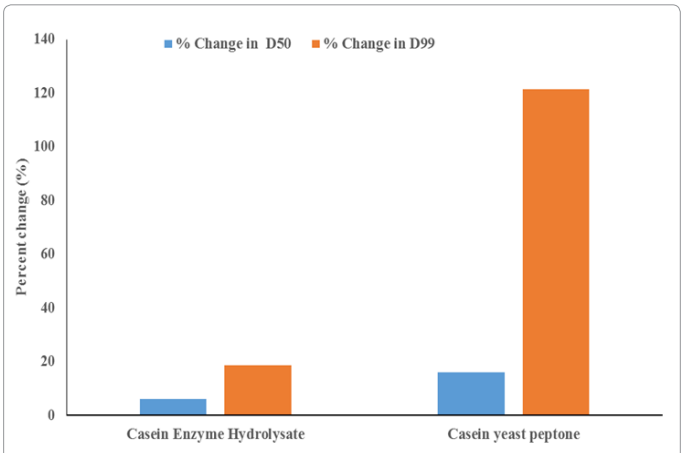

Figure 4: Percentage change between particle size between Control and Treated samples.

Material	Surface area		
	Control (m^2/g)	Treated (m^2/g)	% Change in surface area
Casein enzyme hydrolysate	0.55	1.00	83.90
Casein yeast peptone	1.21	1.12	-7.30

Table 1: Surface area analysis of Casein enzyme hydrolysate and Casein yeast peptone.

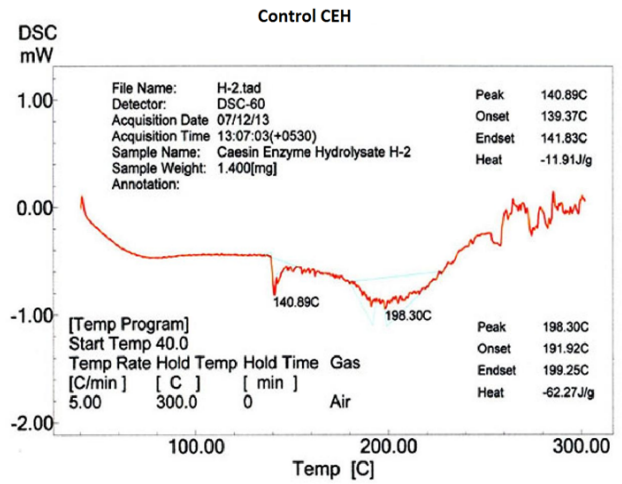

Figure 5a: DSC thermogram of Control casein enzyme hydrolysate.

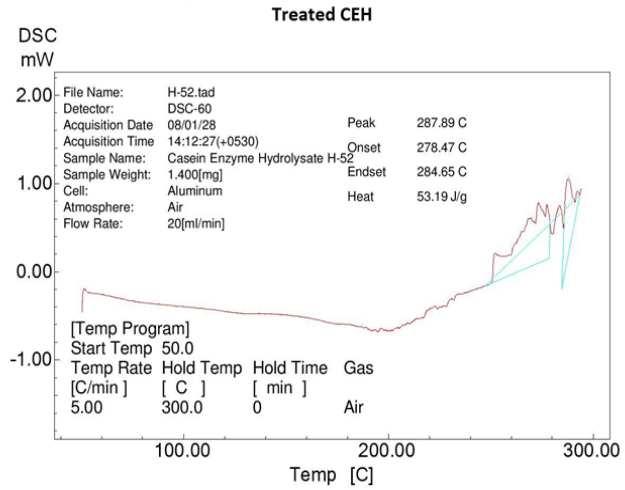

Figure 5b: DSC thermogram of Treated casein enzyme hydrolysate.

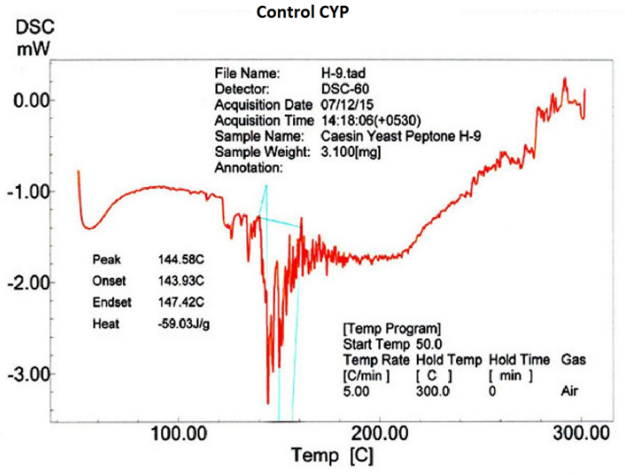

Figure 6a: DSC thermogram of Control casein yeast peptone.

Thermo Gravimetric Analysis (TGA)

TGA analysis provides information about thermal stability of the sample. TGA thermogram of control and treated samples of CEH is presented in Figure 7a and 7b respectively. The control CEH sample showed (Figure 7a) single step thermal degradation which started at 170°C and stopped at 240°C. The derivative thermogravimetry (DTG) showed maximum thermal decomposition temperature at 209°C in control sample. TGA thermogram of treated sample (Figure 7b) showed two step thermal decomposition pattern. In the first step, the sample started to degrade at 190°C and ended at 240°C. During this event the sample lost 12.4% of its original weight. The second step commenced at 260°C and ended at 380°C. The DTG analysis showed a maximum thermal decomposition peak at 217°C in treated sample. The increase in maximum thermal decomposition peak in treated sample probably enhanced the thermal stability as compared to control. It is presumed that biofield treatment has probably induced strong hydrogen bonds in treated CEH sample which raised the decomposition temperature of the sample. It is worthwhile to note here that the FTIR spectrum (Figure 1b) of treated CEH showed hydrogen bonding in the sample. This is also well supported by DSC results.

TGA thermogram of CYP (control and treated) sample is presented in Figure 8a and 8b. The thermal decomposition of the control CYP (Figure 8a) started at 180°C and ended at 228°C. The sample has showed maximum thermal decomposition at 202°C. During this thermal process sample lost 11.26% of its original weight. The comparative evaluation of DTG peaks showed that after biofield treatment the thermal stability of the treated CYP (216°C) (Figure 8b) is found to be increased as compared to control (202°C). This shows the enhanced thermal stability of the treated CYP sample.

Conclusion

This study showed the influence of biofield treatment on the physical and thermal properties of the CEH and CYP. Biofield treatment did cause a significant change in structure characterization, along with an increase in particle size, melting temperature and maximum decomposition temperature as compared to control sample, which were analyzed by standard techniques. Hence we postulate that the biofield treated organic protein products (CEH and CYP) could be used either as an interesting matrix for drug delivery or as a medium for cell culture research.

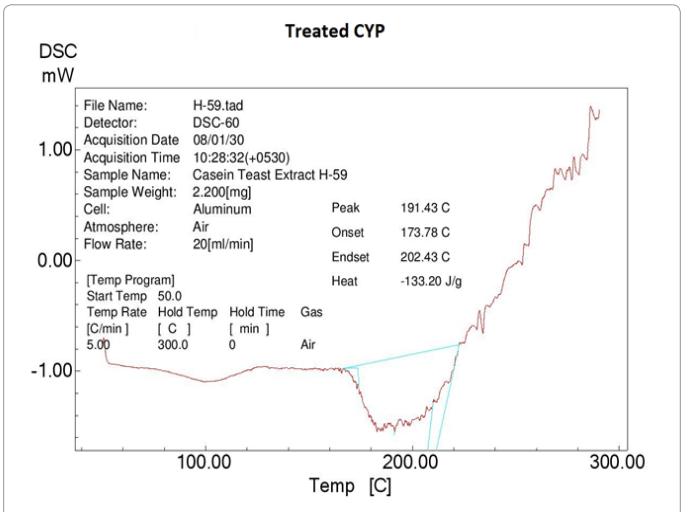

Figure 6b: DSC thermogram of Treated casein yeast peptone.

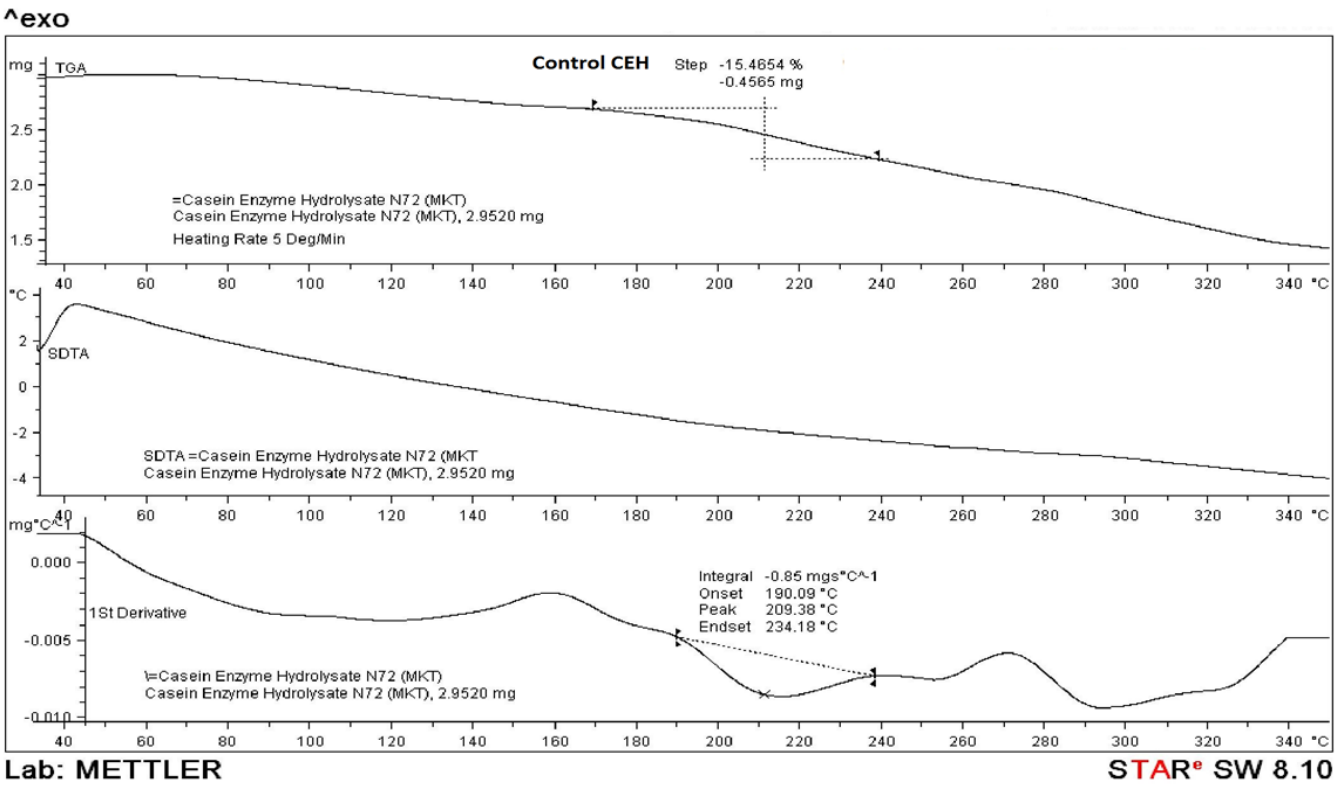

Figure 7a: DTGA thermogram of Control casein enzyme hydrolysate.

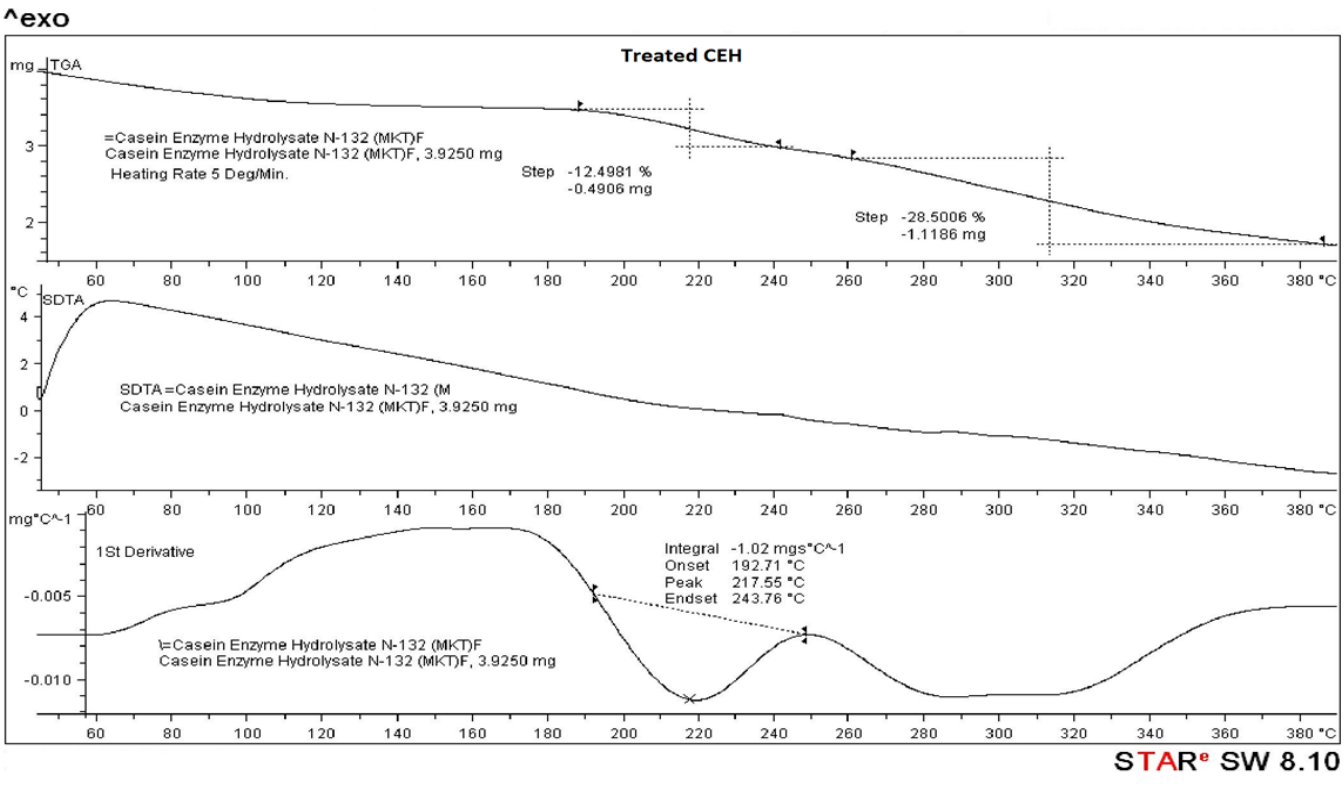

Figure 7b: TGA thermogram of Treated casein enzyme hydrolysate.

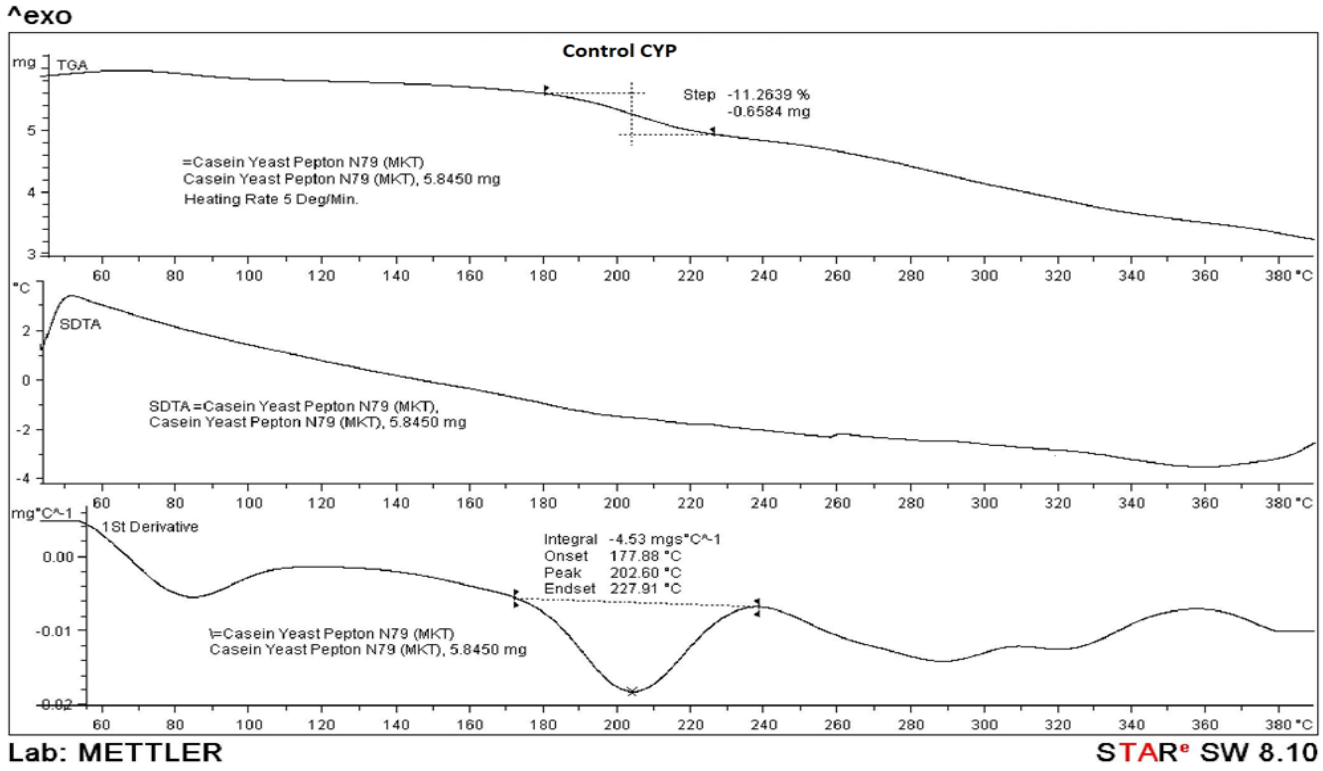

Figure 8a: TGA thermogram of Control casein yeast peptone.

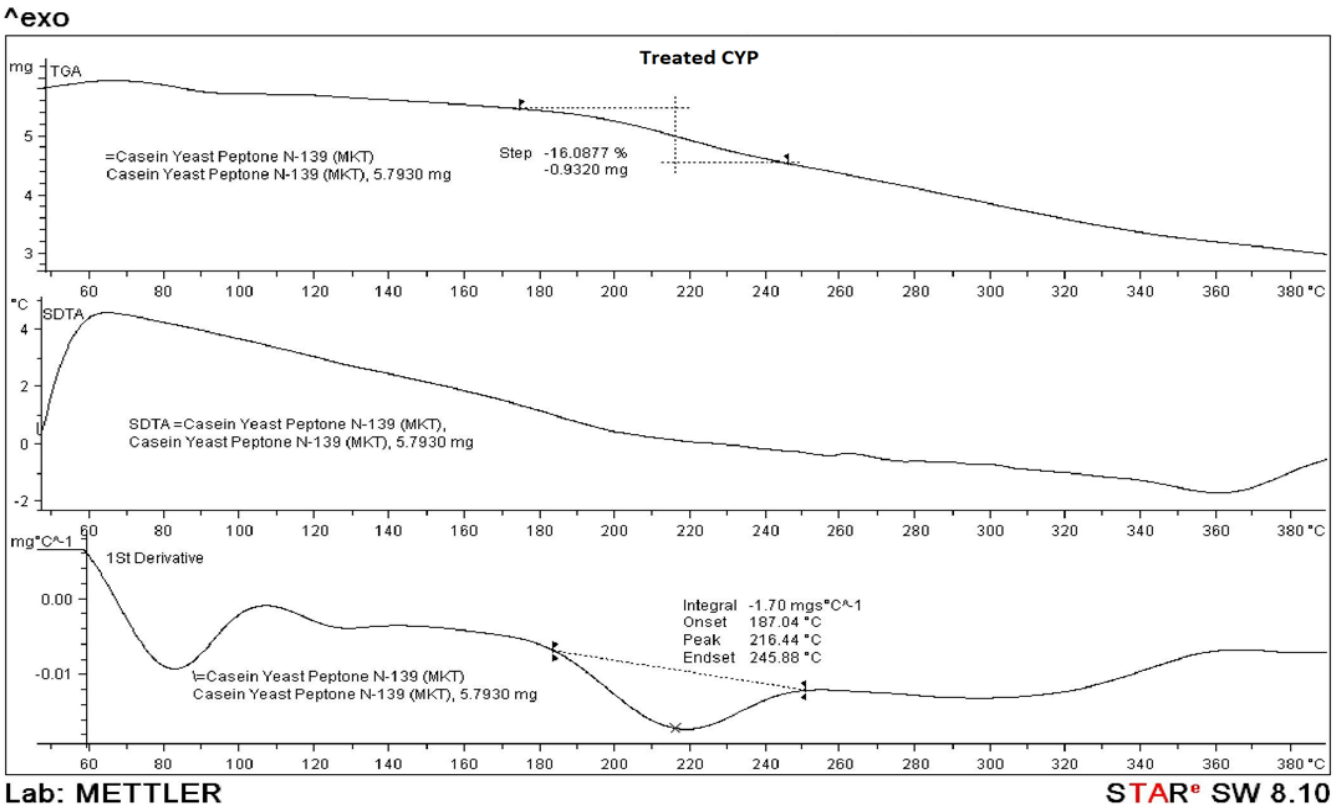

Figure 8b: TGA thermogram of Treated casein yeast peptone.

References

1. Elzoghby AO, Abo El-Fotoh WS, Elgindy NA (2011) Casein-based formulations as promising controlled release drug delivery systems. Journal of Controlled Release 153: 206-216.
2. Lewis DH (1990) Biodegradable Polymers as Drug Delivery Systems. New York: Marcel Dekker. 75: 1-18
3. Bryant CM, McClement DJ (1998) Molecular basis of protein functionality with special consideration of cold-set gels derived from heat-denatured whey. Trends in Food Science & Technology 9: 143-151.
4. Clark AH (1998) Gelation of globular proteins: Functional Properties of Food Macromolecules. Gaithersburg MD: Aspen.
5. Dickinson E. (2003) Colloidal aggregation: mechanism and implications: Food Colloids, Biopolymers and Materials. Cambridge: Royal Society of Chemistry.
6. Walstra P (2003) Studying food colloids: past, present and future: Food Colloids, Biopolymers and Materials. Cambridge: Royal Society of Chemistry.
7. Chen L, Remondetto GE, Subirade M (2006) Food protein-based materials as nutraceutical delivery systems. Trends in Food Science & Technology 17: 272-283.
8. Chen L, Subirade M (2008) Food-protein-derived materials and their use as carriers and delivery systems for active food components. Delivery and Controlled Release of Bioactives in Foods and Nutraceuticals. UK: Woodhead Publishing Ltd.
9. Panyam KD, Kilara Arun (2003) Peptides from milk proteins and their properties. Critical Reviews in Food Science and Nutrition 43: 607-633.
10. Korhonen H, Pihlanto A (2003) Bioactive peptides: new challenges and opportunities for dairy industry. Australian Journal of Dairy Technology 58: 129-134.
11. Livney YD (2010) Milk proteins as vehicles for bioactives. Current Opinion in Colloid & Interface Science 15: 73-83.
12. Wang J, Su Y, Jia F, Jin H (2013) Characterization of casein hydrolysates derived from enzymatic hydrolysis. Chemistry Central Journal 7: 62.
13. Myers R (2003) The basics of chemistry. Westport, Connecticut, London: Greenwood Press.
14. Trivedi MK, Tallapragada RR (2008) A transcendental to changing metal powder characteristics. Metal Powder Report 63: 22- 28 31.
15. Dabhade VV, Tallapragada RR, Trivedi MK (2009) Effect of external energy on atomic, crystalline and powder characteristics of antimony and bismuth powders. Bulletin of Materials Science 32:471-479.
16. Trivedi MK, Tallapragada RR (2009) Effect of super consciousness external energy on atomic, crystalline and powder characteristics of carbon allotrope powders. Materials Research Innovations 13- 473-480.
17. Trivedi MK, Patil S, Tallapragada RM (2012) Thought Intervention through Biofield Changing Metal Powder Characteristics Experiments on Powder Characterisation at a PM Plant , Future Control and Automation Lecture Notes in Electrical Engineering Volume 17: 247-252 .
18. Trivedi MK, Patil S, Tallapragada RM (2013) Effect of Biofield Treatment on the Physical and Thermal Characteristics of Vanadium Pentoxide Powders. Journal of Material Sciences & Engineering S11:001.
19. Trivedi MK, Patil S, Tallapragada RM (2013) Effect of bio field treatment on the physical and thermal characteristics of Silicon, Tin and Lead powders. Journal of Material Sciences & Engineering 2:125.
20. Trivedi MK, Patil S, Tallapragada RM (2014) Atomic, Crystalline and Powder Characteristics of Treated Zirconia and Silica Powders. J Material Sci Eng 3: 144.
21. Trivedi MK, Patil S, Tallapragada RMR (2015) Effect of Biofield Treatment on the Physical and Thermal Characteristics of Aluminium Powders. Industrial Engineering & Management 4:151.
22. Shinde V, Sances F, Patil S, Spence A (2012) Impact of Biofield Treatment on Growth and Yield of Lettuce and Tomato. Australian Journal of Basic and Applied Sciences 6: 100-105
23. Sances F, Flora E, Patil S, Spence A, Shinde V (2013) Impact of Biofield Treatment on Ginseng and Organic Blueberry Yield. AGRIVITA, Journal of Agricultural Science 35: 1991
24. Lenssen AW (2013) Biofield and Fungicide Seed Treatment Influences on Soybean Productivity, Seed Quality and Weed Community. Agricultural Journal 8: 138-143.
25. Altekar N, Nayak G (2015) Effect of Biofield Treatment on Plant Growth and Adaptation. Journal of Environment and Health sciences 1: 1-9
26. Trivedi M, Patil S (2008) Impact of an external energy on Staphylococcus epidermis [ATCC –13518] in relation to antibiotic susceptibility and biochemical reactions - An experimental study. Journal of Accord Integrative Medicine 4: 230-235.
27. Trivedi M, Patil S (2008) Impact of an external energy on Yersinia enterocolitica [ATCC –23715] in relation to antibiotic susceptibility and biochemical reactions: An experimental study. The Internet Journal of Alternative Medicine 6.
28. Trivedi M, Bhardwaj Y, Patil S, Shettigar H, Bulbule A (2009) Impact of an external energy on Enterococcus faecalis [ATCC – 51299] in relation to antibiotic susceptibility and biochemical reactions - An experimental study. Journal of Accord Integrative Medicine 5: 119-130.
29. Patil SA, Nayak GB, Barve SS, Tembe RP, Khan RR (2012) Impact of Biofield Treatment on Growth and Anatomical Characteristics of Pogostemon cablin (Benth.). Biotechnology 11:154-162
30. Colthup NB, Daly LH, Wiberley SE (1975) Introduction to Infrared and Raman Spectroscopy. New York: Academic Press.
31. Barth A (2007) Infrared spectroscopy of proteins. Biochimica et Biophysica Acta (BBA)-Bioenergetics, 1767: 1073-1101.
32. Torii H, Tatsumi T, Tasumi M (1998). Effects of hydration on the structure, vibrational wavenumbers, vibrational force field and resonance Raman intensities of N-methylacetamide. Journal of Raman Spectroscopy 29: 537-546.
33. Mennucci B, Martinez JM (2005) How to model solvation of peptides? Insights from a quantum-mechanical and molecular dynamics study of N-methylacetamide. I. Geometries, infrared, and ultraviolet spectra in water. The Journal of Physical Chemistry B 109: 9818-9829.
34. Bendz D, Tuchsen PL, Christensen TH (2007) The dissolution kinetics of major elements in municipal solid waste incineration bottom ash particles. Journal of Contaminant Hydrology 94: 178-194.
35. Chandler AJ, Eighmy TT, Hartlen J, Hjelmer O, Kosson DS, et al. (1997) Municipal solid waste combustion residues: the international ash working group: Studies in Environmental Science. Amsterdam: Elsevier science.